

## Supporting Information

# Co<sub>2</sub>P Quantum Dot Embedded N, P Dual-doped Carbon Self-supported Electrodes with flexible and binder-free properties for Efficient Hydrogen Evolution Reaction

Chengtian Zhang<sup>a</sup>, Zonghua Pu<sup>a</sup>, Ibrahim Saana Amiinu<sup>a</sup>, Yufeng Zhao<sup>b</sup>, Jiawei Zhu<sup>a</sup>, Yongfu Tang<sup>b</sup>  
and Shichun Mu<sup>a,\*</sup>

<sup>a</sup>State Key Laboratory of Advanced Technology for Materials Synthesis and Processing, Wuhan University of Technology, Wuhan 430070, China

<sup>b</sup>Key Laboratory of Applied Chemistry, Yanshan University, Qinhuangdao 066004, China

E-mail: [msc@whut.edu.cn](mailto:msc@whut.edu.cn)

## Experimental section

### Materials

Aniline, H<sub>2</sub>SO<sub>4</sub> and ethanol were purchased from Aladdin Reagents Ltd. (China). HCl and HNO<sub>3</sub> were purchased from Beijing Chemical Works Ltd. Co(NO<sub>3</sub>)<sub>2</sub>·6H<sub>2</sub>O was purchased from Xinglong Chemical Corp. Ltd. Phytic acid (PA), Pt/C (20 wt. %) and Nafion (5 wt. %) were purchased from Sigma-Aldrich. All the reagents were analytical grade and used without further treatments. The deionized water used throughout the whole experimental process was purified through a Millipore system.

**Preparation of carbon cloth (CC):** CC was cleaned with mixed aqueous solutions of HCl (19 wt. %) and HNO<sub>3</sub> (10 wt. %), followed by washing with deionized water repeatedly.

**Preparation of Co<sub>2</sub>P@NPC:** The preparation of Co<sub>2</sub>P@NPC was obtained by a simple electrodeposition in a three-electrode system consisting of carbon cloth (CC) as working electrode, Ag/AgCl as reference electrode and carbon rod as count electrode at room temperature. The PANI-PA was electropolymerized onto the CC in the electrolyte. The solution was formed by dissolving 8 mL HCl in 50 mL H<sub>2</sub>O and then adding 4.6 g aniline and 10 g phytic acid under stirring for 30 minutes. A potential of 0.8 V was constantly applied to the working electrode for 30 min. And then, PANI-PA/CC was washed with deionized water, followed by drying at 60 °C for half an hour and then immersed in Co(NO<sub>3</sub>)<sub>2</sub>·6H<sub>2</sub>O solution at 40 °C for 2 h, followed by drying at 80 °C for 4 h. A temperature programmed reduction process was then carried out at 700, 800, 900 °C in H<sub>2</sub> for 2h. The heating rate is 5 °C per min. After cooling down to room temperature, the samples were entirely transformed into N, P co-doped carbon structure. The NPC was prepared in a similar way without the soaking step.

### Structural characterizations

Powder X-ray diffraction (XRD) patterns were collected on a Rigaku X-ray diffractometer equipped with a Cu K $\alpha$  radiation source. The morphology and structure were characterized by scanning electron microscopy (SEM: XL30 ESEM FEG) and transmission electron microscopy (TEM: JEM-2100F). X-ray photoelectron spectroscopy (XPS) was performed on an ESCALABMK II X-ray photoelectron spectrometer. Raman shifts were recorded on a LabRAM Aramis Raman spectrometer instrument using an Ar ion laser with an excitation wavelength of 633 nm.

## Electrochemical measurements

All electrochemical measurements are performed on a CHI 660E electrochemical analyzer (CH Instruments, Inc., Shanghai) in a standard three-electrode with a two-compartment cell. The acidic (0.5 M H<sub>2</sub>SO<sub>4</sub>) and electrochemical measurements were performed using a saturated calomel electrode (SCE) as the reference electrode. The graphite rod was used as the counter electrode in all measurements. Polarization data were obtained at a scan rate of 2 mV s<sup>-1</sup>. In all measurements, the reference electrode was calibrated with respect to the reversible hydrogen electrode (RHE). All polarization curves were iR-corrected. Electrochemical impedance spectroscopy (EIS) measurements were carried out in the frequency range of 100 kHz–0.01 Hz.

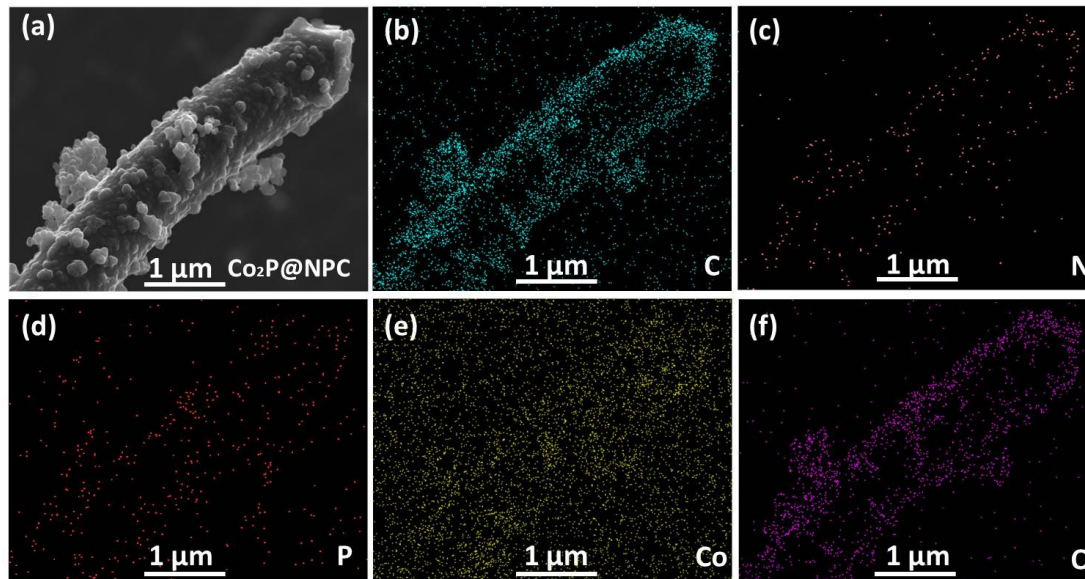


Figure S1. EDX element mapping images of (a) Co<sub>2</sub>P@NPC-800 coated on CC, (b) C, (c) N, (d) P, (e) Co and (f) O.

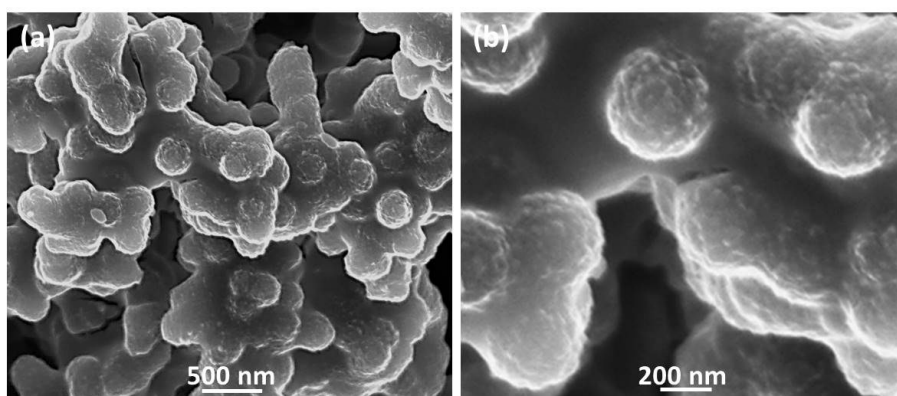


Figure S2. (a, b) SEM images of  $\text{Co}_2\text{P@NPC-700}$ .

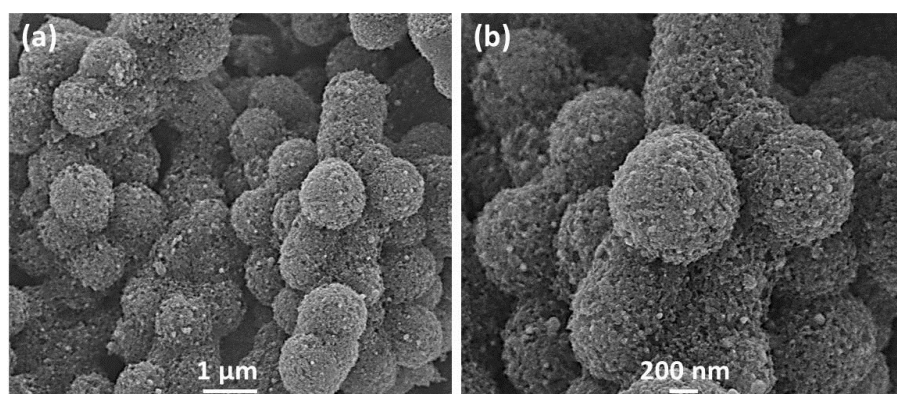


Figure S3. (a, b) SEM images of  $\text{Co}_2\text{P@NPC-900}$ .

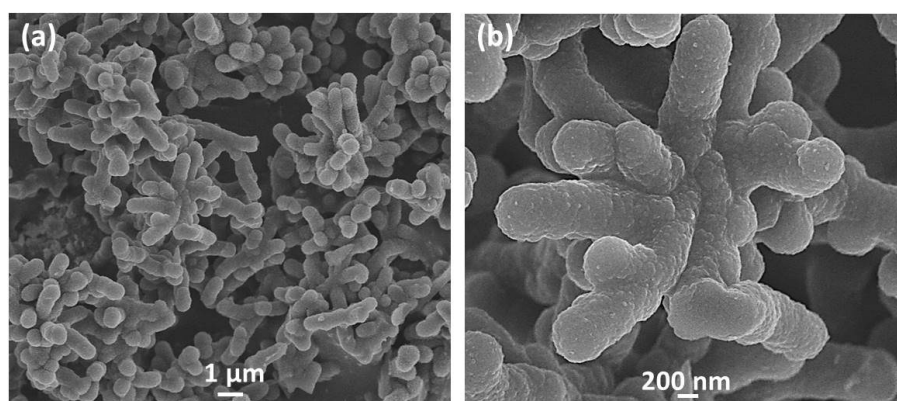


Figure S4. (a, b) SEM images of NPC.

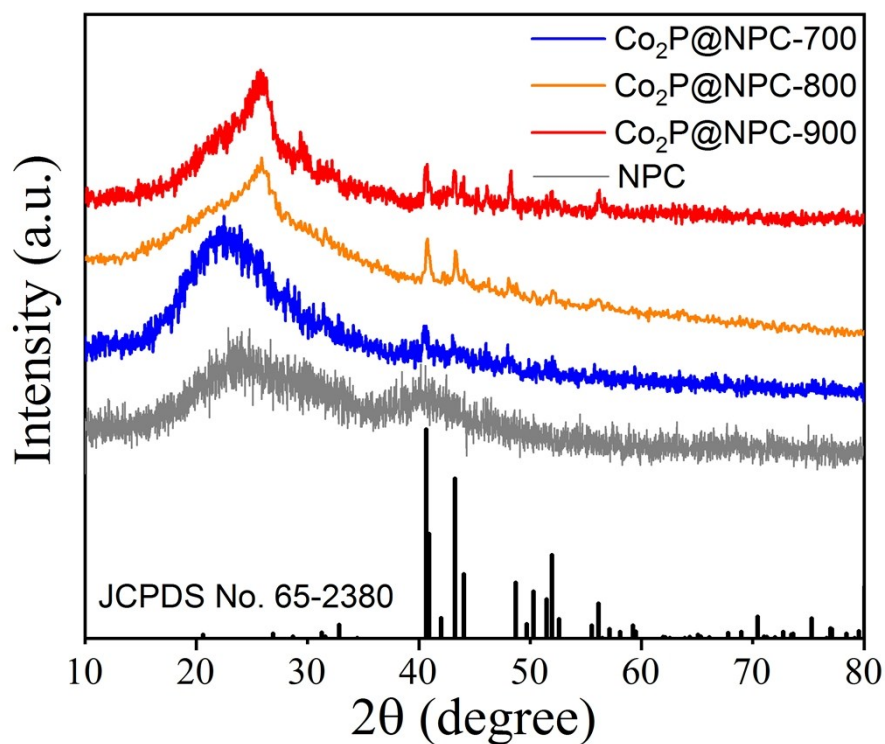


Figure S5. XRD pattern of NPC, Co<sub>2</sub>P@NPC-700, Co<sub>2</sub>P@NPC-800 and Co<sub>2</sub>P@NPC-900.

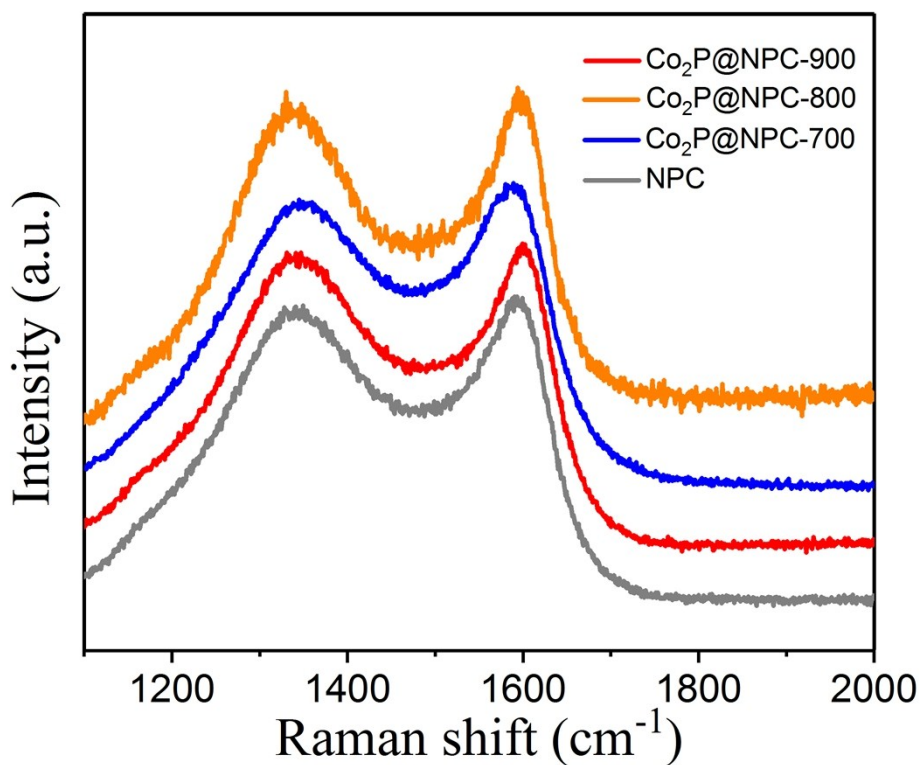


Figure S6. Raman spectrum of NPC ( $I_D/I_G=0.9771$ ), Co<sub>2</sub>P@NPC-700 ( $I_D/I_G=0.9620$ ), Co<sub>2</sub>P@NPC-800 ( $I_D/I_G=0.9914$ ) and Co<sub>2</sub>P@NPC-900 ( $I_D/I_G=0.9764$ ).

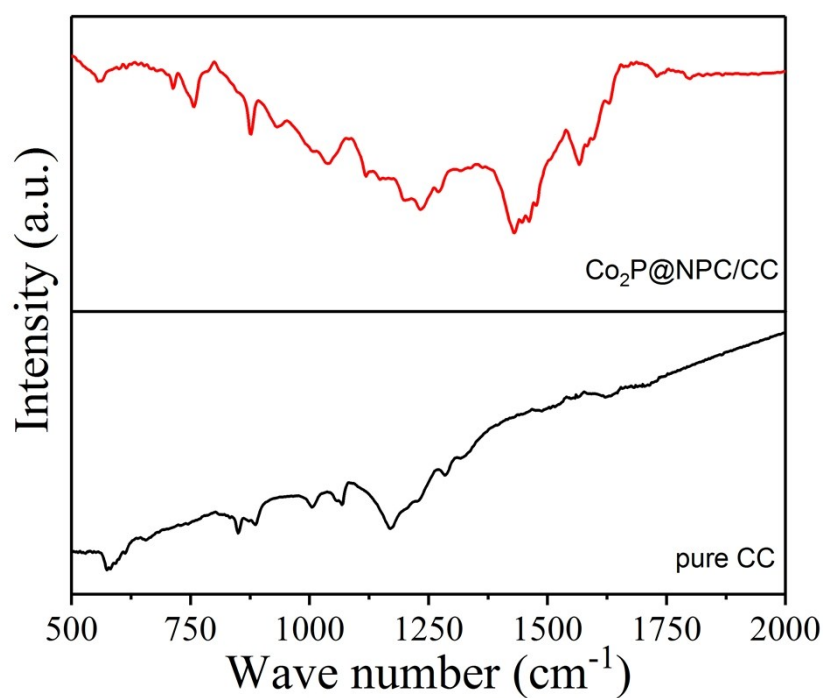


Figure S7. FTIR spectrum of  $\text{Co}_2\text{P@NPC}$  and the pure CC.

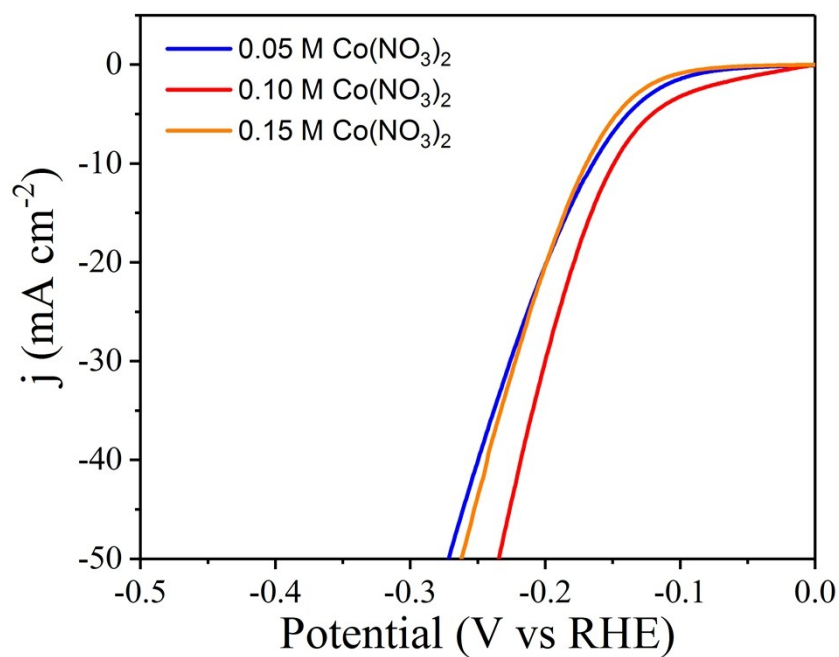


Figure S8. Effect of metal contents on the electrocatalytic activity of  $\text{Co}_2\text{P@NPC}$ . Polarization curves (without iR-correction) for HER were carried out in 0.5 M  $\text{H}_2\text{SO}_4$  for  $\text{Co}_2\text{P@NPC-800}$  with different Co contents.

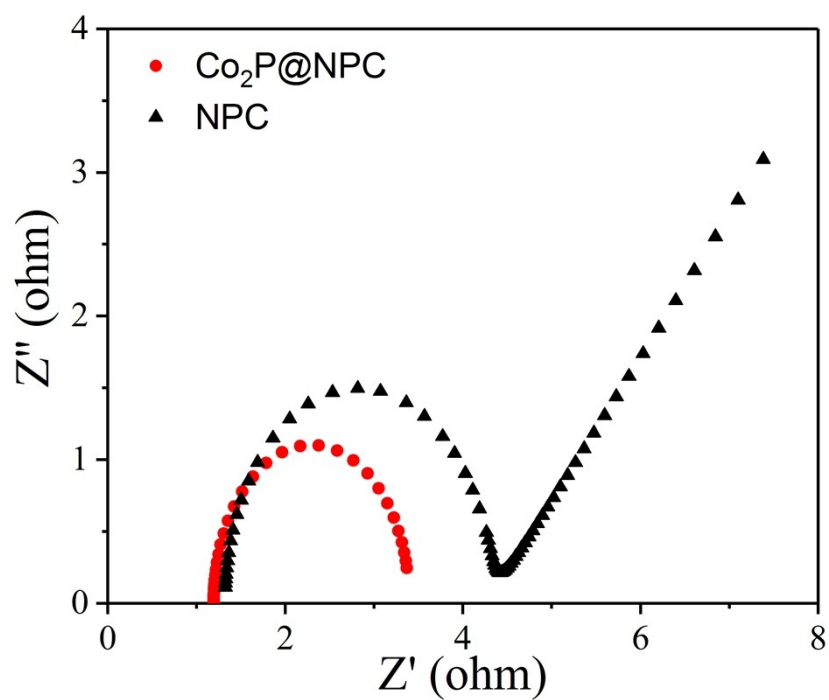


Figure S9. Nyquist plot of  $\text{Co}_2\text{P@NPC}$  and NPC.

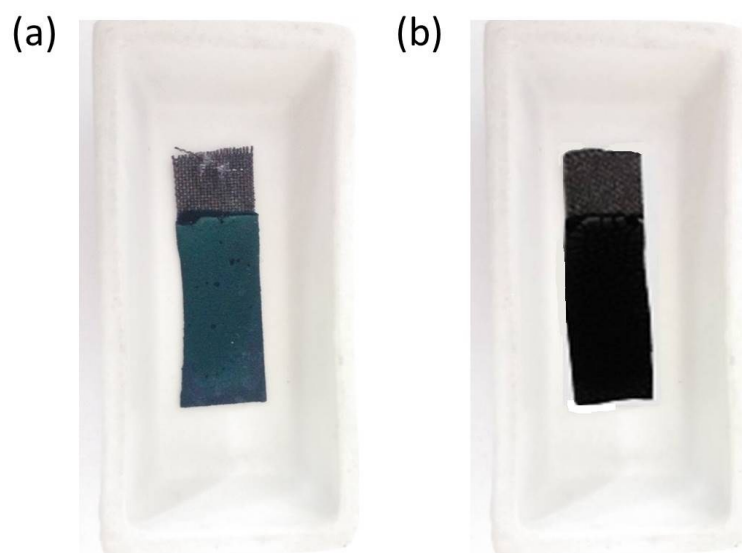


Figure S10. Photograph of (a) the precursor coated on CC after electrolytic deposition and (b) the  $\text{Co}_2\text{P@NPC/CC}$ .

**Table S1.** Comparison of HER performance of Co<sub>2</sub>P@NPC with other recently reported catalysts in 0.5 M H<sub>2</sub>SO<sub>4</sub>.

Catalyst	Current density ( <i>j</i> , mA cm <sup>-2</sup> )	Overpotential at the corresponding <i>j</i> (mV)	Ref.
Co <sub>2</sub> P@NPC	10	116	This work
CoP/CNT	10	122	[1]
CoP hollow NPs	20	80	[2]
CoP nanotubes	10	129	[3]
Co <sub>2</sub> P/Ti	10	100	[4]
Co <sub>2</sub> P@N,P- PCN/CNTs	10	126	[5]
Co <sub>2</sub> P@NPG	10	103	[6]
CoP/CNT	10	122	[7]
Ni <sub>2</sub> P	10	137	[8]
FeP NPs@NC	10	130	[9]
CoP/rGO	10	105	[10]
CoP Hollow Polyhedron	10	159	[11]
CoP/carbon nanotubes	10	139	[12]
Mo <sub>2</sub> C/CC	20	193	[13]
Porous Ni <sub>2</sub> P Polyhedrons	10	158	[14]
Co <sub>2</sub> P/C	10	125	[15]

**Table S2.** Comparison of HER performance of Co<sub>2</sub>P@NPC with other recently reported catalysts in 1 M KOH.

Catalyst	Current density ( <i>j</i> , mA cm <sup>-2</sup> )	Overpotential at the corresponding <i>j</i> (mV)	Ref.
Co <sub>2</sub> P@NPC	10	129	This work
CoP/CC	10	209	[16]
CoP@NC	10	210	[17]
FeP NPs/CC	10	218	[18]
Co-NRCNTs	10	370	[19]
Co <sub>2</sub> P@NPG	10	165	[6]
CoP <sub>2</sub> /RGO	10	88	[20]
Co <sub>2</sub> P nanorods	20	171	[21]
FeP NTs/CC	10	120	[22]
Co-P film	10	94	[23]
CoP <sub>3</sub>	10	119	[24]
NiCoP quasi-hollow nanocubes	10	150	[25]
NiCoP Hollow QuasiPolyhedra	10	124	[26]
CuCoP/nitrogen-doped carbon	10	220	[27]
Ni-Co mixed phosphide/nitrogen-doped carbon	10	116	[28]
FeP <sub>2</sub> /Fe foil	10	189	[29]
Co@NG	10	337	[30]

**Table S3.** Elemental content analysis result of Co<sub>2</sub>P@NPC

Element	Mass Conc (wt. %)
P	2.63
Co	6.10
C	83.28
N	3.16



## Reference:

1. Q. Liu, J. Tian, W. Cui, P. Jiang, N. Cheng, A. M. Asiri and X. Sun, *Angew. Chem. Inter. Ed.*, 2014, **53**, 6828–6832.
2. E. Popczun, C. Read, C. Roske, N. Lewis and R. Schaak, *Angew. Chem. Int. Ed.*, 2014, **53**, 5531–5534.
3. H. Du, Q. Liu, N. Cheng, A. M. Asiri, X. Sun and C. Li, *J. Mater. Chem. A*, 2014, **2**, 14812–14816.
4. J. F. Callejas, C. G. Read, E. J. Popczun, J. M. McEnaney and R. E. Schaak, *Chem. Mater.*, 2015, **27**, 3769–3774.
5. X. Z. Li, Y. Y. Fang, F. Li, M. Tian, X. F. Long, J. Jin and J. T. Ma, *J. Mater. Chem. A*, 2016, **4**, 15501–15510.
6. M. Zhuang, X. Qu, Y. Dou, L. Zhang, Q. Zhang, R. Wu, Y. Ding, M. Shao and Z. Luo, *Nano Lett.*, 2016, **16**, 4691–4698.
7. Q. Liu, J. Tian, W. Cui, P. Jiang, N. Cheng, A. M. Asiri and X. Sun *Angew. Chem. Int. Ed.*, 2014, **53**, 6710–6714.
8. Y. Pan, Y. Liu, J. Zhao, K. Yang, J. Liang, D. Liu, W. Hu, D. Liu, Y. Liu and C. Liu, *J. Mater. Chem. A*, 2015, **3**, 1656–1665.
9. Z. Pu, I. S. Amiinu, C. Zhang, M. Wang, Z. Kou and S. Mu, *Nanoscale*, 2017, **9**, 3555–3560.
10. L. Jiao, Y. Zhou and H. Jiang, *Chem. Sci.*, 2016, **7**, 1690–1695.
11. M. Liu and J. Li, *ACS Appl. Mater. Inter*, 2016, **8**, 2158–2165.
12. C. Wu, Y. Yang, D. Dong, Y. Zhang and J. Li, *Small*, 2017, **13**.
13. M. F. H. Chen, Y. Wu, L. Feng, Y. Liu, G. Li and X. Zou, *J. Mater. Chem. A*, 2015, **3**, 16320–16326.
14. L. Yan, P. Dai, Y. Wang, X. Gu, L. Li, L. Cao and Zhao, X, *ACS Appl. Mater. Inter*, 2017, **9**, 11642–11650.
15. A. Dutta, A. K. Samantara, S. K. Dutta, B. K. Jena and N. Pradhan, *ACS Energy Lett*, 2016, **1**, 169–174.
16. J. Tian, Q. Liu, A. M. Asiri and X. Sun, *J. Am. Chem. Soc.*, 2014, **136**, 7587–7590.
17. J. Wang, D. Gao, G. Wang, S. Miao, H. Wu, J. Li and X. Bao, *J. Mater. Chem. A*, 2014, **2**, 20067–20074.
18. Y. Liang, Q. Liu, A. M. Asiri, X. Sun and Y. Luo, *ACS Catal.*, 2014, **4**, 4065–4069.
19. X. Zou, X. Huang, A. Goswami, R. Silva, B. R. Sathe, E. Mikmekova and T. Asefa, *Angew. Chem. Int. Ed.*, 2014, **126**, 4461–4465.
20. J. Wang, W. Yang and J. Liu, *J. Mater. Chem. A*, 2016, **4**, 4686–4690.
21. J. Chang, Y. Xiao, M. Xiao, J. Ge, C. Liu and W. Xing, *ACS Catal.*, 2015, **5**, 6874–6878.
22. Y. Yan, B. Xia, X. Ge, Z. Liu, A. Fisher and X. Wang, *Chem. Eur. J.*, 2015, **21**, 18062–18067.
23. N. Jiang, B. You, M. Sheng and Y. Sun, *Angew. Chem. Int. Ed.*, 2015, **54**, 6251–6254.
24. T. Wu, M. Pi, D. Zhang and S. Chen, *J. Mater. Chem. A*, 2016, **4**, 14539–14544.
25. Y. Feng, X. Y. Yu, and U. Paik, *Chem. Commun*, 2016, **52**, 1633–1636.
26. Li, Y., Liu, J., Chen, C., Zhang, X. and Chen, J., *ACS Appl. Mater. Inter*, 2017, **9**, 5982–5991.
27. J. Song, C. Zhu, B. Xu, S. Fu, M. H. Engelhard, R. Ye, D. Du, S. P. Beckman and Y. Lin, *Adv. Energy. Mater.*, 2017, **7**.

28. L. Han, T. Yu, W. Lei, W. Liu, K. Feng, Y. Ding, G. Jiang, P. Xu and Z. Chen, *J. Mater. Chem. A*, 2017, **5**, 16568-16572.
29. Y. Yan, B. Xia, X. Ge, Z. Liu, A. Fisher and X. Wang, *Chem. Eur. J.*, 2015, **21**, 18062-18067
30. H. Fei, Y. Yang, Z. Peng, G. Ruan, Q. Zhong, L. Li, E. L. G. Samue and J. M. Tour, *ACS Appl. Mater. Inter*, 2015, **7**, 8083–8087.